1
2
3
4
5
6
7
8
9
10
11
12
13
14
15
16
17
18
19
20
21
22
23
24
25
26
27
28
29
30
31
32
33
34
35
36
37
38
39
40
41
42
43
44
45
46
47
48
49
50
51
52
53
54
55
56
57
58
59
60

Quasi-static characterisation and impact testing of auxetic foam for sports safety applications

Olly Duncan[1], Leon Foster[2], Terry Senior[2], Andrew Alderson[1,3], Tom Allen[2,4]

[1] Materials and Engineering Research Institute

Faculty of Arts, Computing, Engineering and Sciences

Sheffield Hallam University

Howard Street, Sheffield S1 1WB UK

Email: A.Alderson@shu.ac.uk

[2] Centre for Sports Engineering Research

Faculty of Health and Wellbeing

Sheffield Hallam University

Howard Street, Sheffield S1 1WB, UK

[3] Author to whom correspondence should be addressed

[4] Present address: School of Engineering, Faculty of Science & Engineering, Manchester Metropolitan University, John Dalton Building, Chester Street, Manchester M1 5GD, UK

Abstract

This study compared low strain rate material properties and impact force attenuation of auxetic foam and the conventional open-cell polyurethane counterpart. This furthers our knowledge with regards to how best to apply these highly conformable and breathable auxetic foams to protective sports equipment. Cubes of auxetic foam measuring 150 x 150 x 150 mm were fabricated using a thermo-mechanical conversion process. Quasi-static compression confirmed the converted foam to be auxetic, prior to being sliced into 20 mm thick cuboid samples for further testing. Density, Poisson's ratio and the stress-strain curve were all found to be dependent on the position of each cuboid from within the cube. Impact tests with a hemispherical drop hammer were performed for energies up to 6 J, on foams covered with a polypropylene sheet between 1 and 2 mm thick. Auxetic samples reduced peak force by ~10 times in comparison to the conventional foam. This work has shown further potential for auxetic foam to be applied to protective equipment, while identifying that improved fabrication methods are required.

Key Words

Negative Poisson's ratio, sport, protection, material, stiffness, force, auxetic

Introduction

Protective equipment for sport and recreation is designed to reduce injuries and discomfort, caused by impacts and collisions [1]. Due to space and weight constraints the complex designs seen in other shock absorbing appliances - such as mechanical suspension systems - cannot be utilised. Protective equipment relies almost entirely on the properties of monolithic materials, which are often foams, covered with a stiff shell to help distribute concentrated loads [2-4]. Any developments in materials which aid energy absorption, peak force

attenuation and indentation resilience are beneficial.

Auxetic (negative Poisson's ratio) foams have the potential to absorb more energy than conventional foams [5-6]. For a comprehensive review of auxetic materials from the late 1980s to 2014 the reader is referred to [7]. A common fabrication method for auxetic foams is the thermo-mechanical process which begins with compression of open-cell foam into a mould, followed by heating close to or beyond the softening temperature so the cell ribs buckle and form a re-entrant structure [5, 8-9]. Volumetric compression ratio (VCR) (initial to final volume) typically falls between 2 to 5 [8]. A final stage of conversion involves annealing below the softening temperature to lock in the re-entrant structure. Irregularities in re-entrant foam structure have been reported with this method [10,11], and chemical-mechanical [12] or mechanical-chemical-thermal [13] processes offer alternatives.

Early studies fabricated and characterised small sized samples of auxetic foam [e.g. 14] (smallest dimension < 25 mm), while more recent work has produced larger samples [e.g. 15-19] (50 mm < smallest dimension < 100 mm) as the research has moved towards applications. Poisson's ratios are typically calculated from true strain measurements, obtained by filming and tracking the location of marks applied to a sample subject to quasi-static tension or compression. Auxetic foams typically have a lower Young's modulus under compression, in comparison to their conventional open-cell counterparts, [14-16, 20], although an increase in stiffness has also been reported in some cases [13, 18 and 19]. The stress-strain curve for auxetic foams under compression typically has an extended region of linear elasticity providing higher resilience [5, 15-17]. Camera or microscope images are often used alongside mechanical tests to identify re-entrant cell structures in converted foams. Previous work has shown inhomogeneity in the structure of converted foam [19]. Cellular

structure (geometry and orientation) contributes significantly to the mechanical properties of a cellular solid [7, 21, 22].

In comparison to their conventional counterparts, auxetic foams exhibit higher indentation resilience during quasi-static tests [15, 23] and lower peak acceleration under impact [16-18]. High-speed video has been used to confirm that lower peak acceleration is due to greater resistance to compression under impact, preventing "bottoming out" as observed with conventional foam [17]. Comparative low-kinetic energy impact testing with a concentrated load has shown peak accelerations around six times lower for auxetic foam, when samples were covered with a thin semi-rigid sheet characteristic of protective equipment [16]. Measurements of Poisson's ratio of auxetic foams during quasi-static compression and drop tower impact testing have provided comparable results [16]. Increasing compressive strain rates have also been shown to increase stiffness and reduce the magnitude of Poisson's ratio of auxetic foams [24].

This paper aims to further investigate the suitability of auxetic foam for use in protective sports equipment, through investigating the effect of scaling the fabrication process to produce larger sized monolithic cubes from which thinner samples can be cut (to reduce fabrication costs compared to producing individual converted thin samples) and investigating the effect of covering sheet thickness on force attenuation for higher energy impacts with a concentrated load.

Methods

The methods were adapted from similar work also using reticulated open-cell polyester-based polyurethane foam [15-17]. Auxetic foam cubes measuring 150 x 150 x 150 mm were

fabricated using a multi-stage thermo-mechanical process employing a compression of each linear dimension to 70% of its unconverted value. No recovery of dimensions was observed in the converted samples over a period of 3 weeks, confirming that the processing conditions employed in the foam conversion process produced stable samples over the timescales of this investigation. Following removal of 25 mm from each face, to eliminate any surface creasing and folding, the resulting 100 x 100 x 100 mm cubes were subject to quasi-static compression to obtain Poisson's ratio, stress-strain curves and Young's moduli. Each cube was then cut into five 100 x 100 x 20 mm cuboidal samples for quasi-static compression and impact testing against unconverted foam samples of the same dimensions. The 100 x 100 x 20 mm sliced samples of converted foam were visibly less dense towards the centre than the edges of foam trimmed from the converted 150 x 150 x 150 mm monolithic cube. Impact tests were performed using an instrumented hemispherical drop hammer with a 1, 1.5 or 2 mm thick polypropylene (PP) sheet (Direct Plastics, PPH/PP-DWST-Homopolymer) placed on top of the foam without any bonding.

The foam was R30FR reticulated open-cell polyester-based polyurethane foam with flame retardant additive, having 30 pores inch^{-1} and a density of 26 to 30 Kg m^{-3}, supplied by Custom Foams in two 215 x 215 x 215 mm cubes. A metal mould, comprising 2 'U'-shaped pieces with enclosed internal dimensions of 150 x 150 x 150 mm, containing the compressed foam was heated at the designated conversion temperature for two 35 minute periods in a conventional oven before annealing at 100°C for 35 minutes. Between each stage the foam was removed from the mould and gently stretched in all three orthogonal planes. One cube was converted at 180°C and the other at 200°C, corresponding to temperatures used previously with smaller sized samples [16-17]. An extended heating time was adopted over the previous work, rather than an increase in temperature, to assist heating of the centre of the

foam and prevention of adhesion of cell ribs caused by over-heating [10].

The quasi-static uniaxial compression tests were performed on specimens in the absence of a PP shell with a universal testing machine (Instron 3369, fitted with a 50 kN load cell and flat compression plates) up to 50% compression at 0.008 s^{-1}. Young's Moduli were obtained from linear regression of stress-strain data up to 10% compression. Four pin heads arranged in a 60 x 60 mm square centred on the cube face (figure 1a) were filmed with a camera (JVC Everio Full HD resolution 1920 x 1080 pixels) and then tracked using a bespoke MATLAB (MathWorks) algorithm to obtain true strains in both directions. Poisson's ratios were obtained from linear regression of the true strain-strain data up to compressive strains of 0.1. Each cube was tested five times with the loading direction aligned with the foam rise direction.

The cubes were then cut into five equal cuboids - with the rise direction through the thickness using a band saw (Bauer Maschinenbau) – and compression tested three times each to obtain stress-strain curves and Poisson's ratio. Due to the reduced thickness of the samples, three pins heads horizontally aligned ~30 mm apart were used to obtain lateral true strain measurements (figure 1b). Compressive axial true strain measurements were obtained from the position data recorded by the test machine. Four unconverted samples of the same sample size were cut from a monolith and compression tested once each to obtain stress-strain curves and Young's modulus. The Poisson's ratio of reticulated open-cell polyester foam has been reported previously in the range 0.29 to 0.43 [13-15]. Given the evident visible variation in foam density throughout the converted monolithic foam cubes, the density of the converted foam was obtained from measurements taken using callipers and scales, and used to obtain the final VCR (of the trimmed cubes and also the sliced samples) by normalising to the value

1
2
3
4
5
6
7
8
9
10

$(28 \pm 1 \ \text{kg m}^{-3})$ measured for the unconverted foam. Through thickness images at a magnification of 4.3 were taken using a LEICA S6D stereoscope to further inspect variations in material structure.
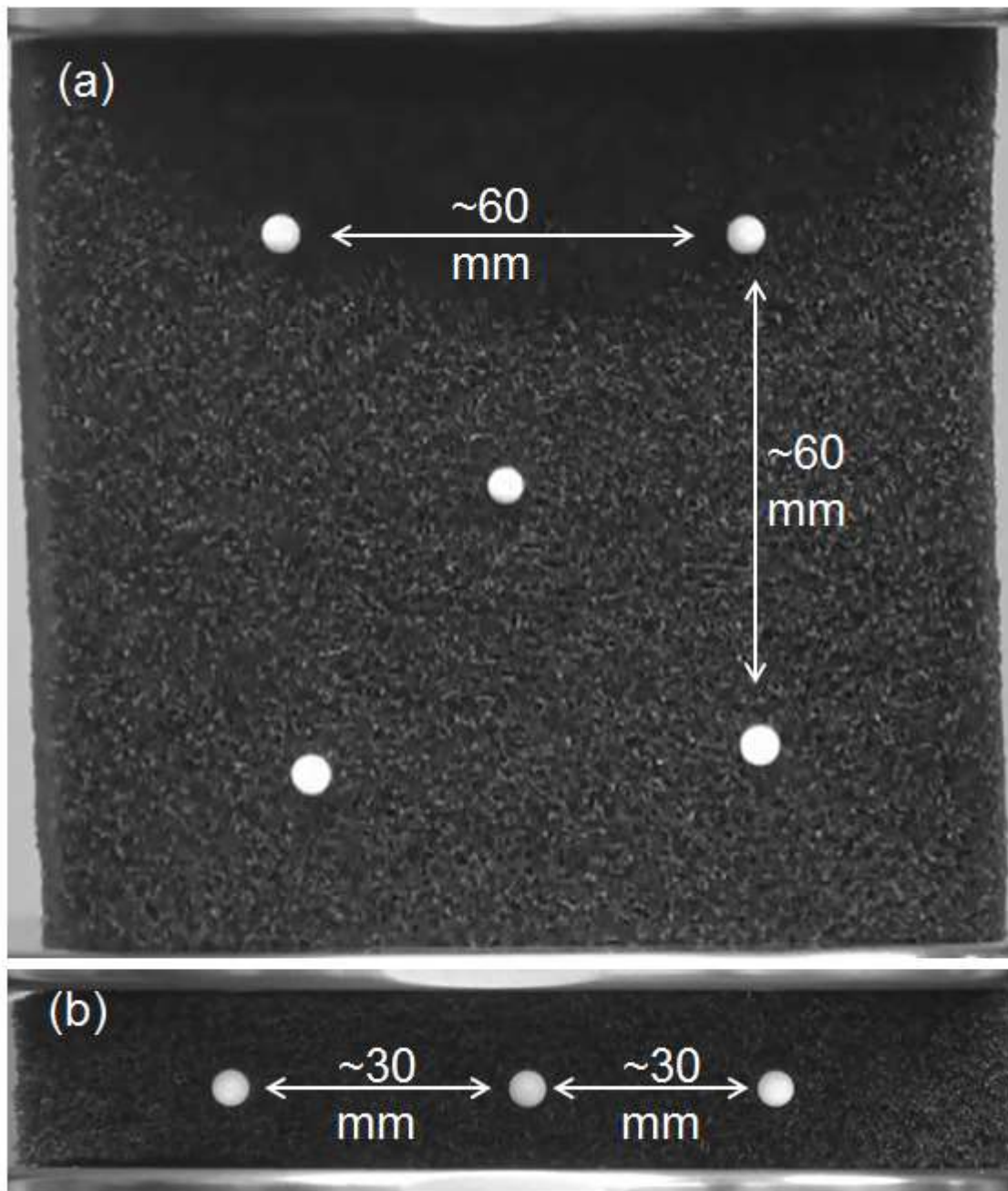

Figure 1 Pin locations for quasi-static compressive tests of: a) 100 x 100 x 100 mm cubes b) 20 x 100 x 100 mm cuboids.

Impact tests were performed for kinetic energies of 4 and 6 J, using a bespoke drop rig [16-17]. The tests were inspired by the British Standard for protective equipment for cricketers

(BS 6183-3:2000), with similar impact energies to the lowest performance level and the same shape hammer, but the sample rested on a flat surface rather than a curved anvil [25]. The drop hammer (2.09 kg and 73 mm diameter hemisphere) was fitted with wireless accelerometers (Analog Devices, ADXL001-5000g & 500g) recording at 10 kHz providing acceleration-time data (DTS SLICEWare Version 1.08.0475). A high-speed video camera (Vision Research, Phantom V4.3) - operating at 10 kHz, with an exposure time of 30 μs and a resolution of 832 x 64 pixels - filmed a marker placed on the drop hammer to enable measurement of displacement and determine the time corresponding to the end of impact. Video footage and accelerometer traces were processed with a bespoke MATLAB algorithm to combine and align the peaks in the displacement and acceleration data strings, with the start of contact identified when acceleration first exceeded 1 g. Visual comparison using the video footage indicated the start of contact could be identified to within 1 ms with this method. The end of the impact was defined as when the drop hammer returned to the height identified as the start of contact. A moving average (up to 11 points) was applied to the displacement data and a low pass Butterworth filter reduced the mostly high frequency noise of motion throughout the accelerometer data.

Results

Figure 2a shows stress-strain curves for the 100 x 100 x 100 mm cubes converted at 180 and 200°C. The cubes exhibited similar stress-strain relationships, although the sample converted at 200°C was slightly stiffer at higher strains (>0.2). Young's modulus was 30 ± 5 kPa (mean $\pm$ standard deviation) for the sample converted at 180°C, with a marginally higher value of 33 ± 4 kPa for the 200°C cube. Figure 2b shows similar lateral strain vs axial strain data for the two cubes, with a relatively linear relationship up to full compression. Poisson's ratio was similar for both cubes, -0.019 ± 0.021 at 180°C and -0.026 ± 0.006 at 200°C. The VCR was

calculated from the density as 1.7 for the trimmed 180°C cube and 1.9 for the trimmed 200°C

cube, which are both lower than the value of 2.9 applied to the untrimmed 150 x 150 x 150

mm sample during conversion. This reduction in internal volumetric compression ratio

(resulting in greater compliance towards the centre of each cube) caused the increased values

for axial compressive true strain in the tracked marker positions (Figure 2b), and is consistent

with the observation that the trimmed edges from the full converted cubes were visibly higher

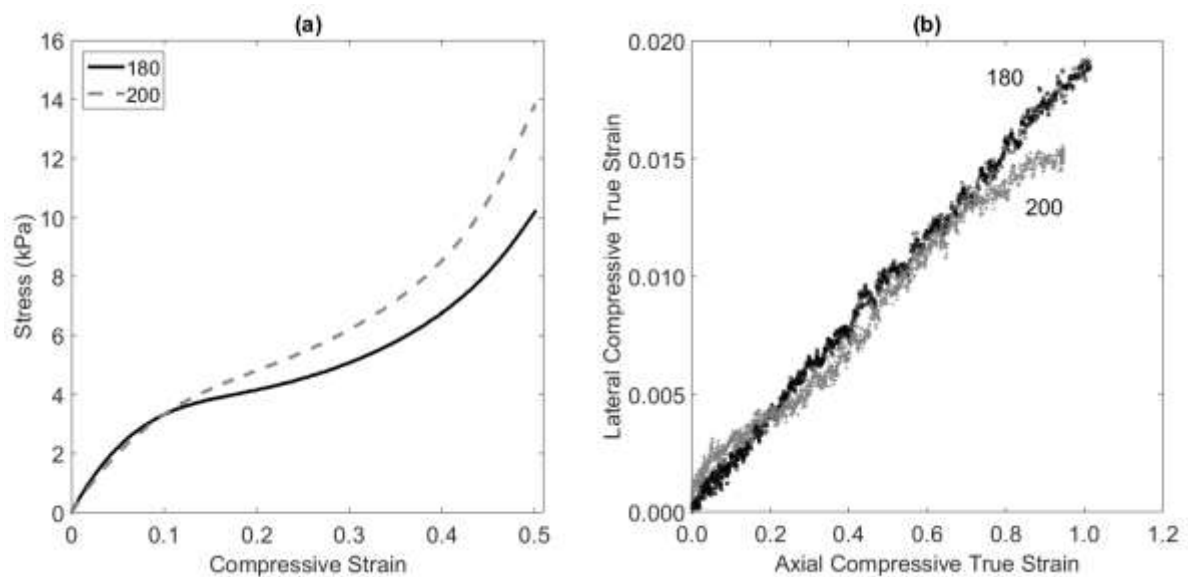density than the trimmed cubes.

Figure 2 Quasi-static compression data for 100 x 100 x 100 mm trimmed cubes cut from 150 x 150 x 150 mm converted

cubes. a) Mean stress-strain data b) true strain-strain data for a test with the loading axis aligned with the rise direction.

Poisson's ratio was -0.019 for the test on the 180°C sample and -0.021 for the 200°C sample.

Figure 3a shows stress-strain curves for the 100 x 100 x 20 mm converted and unconverted

samples. The unconverted foam exhibited the classic relationship [21], with a high stiffness

linear elastic region (E = 43 ± 9 kPa) followed by a plateau beginning at ~10% compression.

This is reflected in the tangent modulus curve in Figure 3b (derived from the slope of the

stress-strain data in Figure 3a), which shows the unconverted foam to have almost zero

stiffness in the region corresponding to 10 to 50 % compression. Samples taken from the top

of the cubes exhibited an extended region of near-linear elasticity until ~40% compression,

followed by progressively increasing stiffness (Figures 3a and 3b). Samples from the centre

exhibited intermediate behaviour, with similar stress-strain curves to those presented for the

cubes in Figure 2a. The converted foam samples are one to two orders of magnitude stiffer

than the unconverted parent foam for compressive strains ranging from 10 to 50%. The

indentation response of a material is dependent on both the Poisson's ratio and Young's

modulus of the material [26]. Hence we expect the increased Young's modulus response of

converted foams at intermediate and higher strains will also be a significant factor, in

addition to the negative Poisson's ratio effect, in the indentation response of the converted
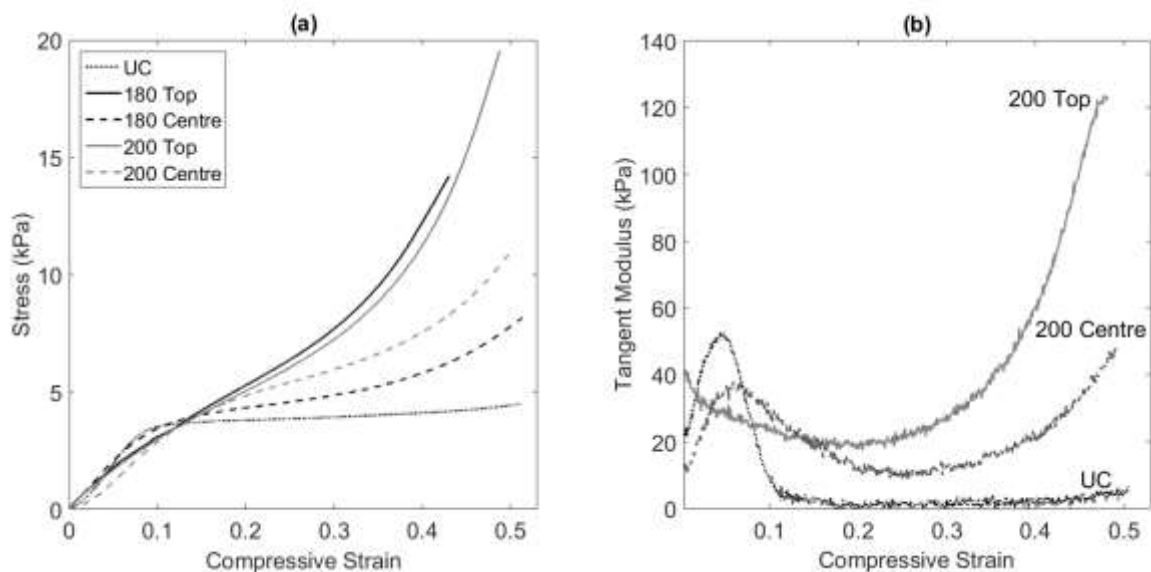
foams.

Figure 3 Quasi-static compression data for the 100 x 100 x 20 mm cuboids cut from the converted cubes. a) Mean stress-strain data, b) tangent modulus of UC and example auxetic samples.

Figure 4a shows a re-entrant cellular foam structure, characteristic of an auxetic foam, for the

sample taken from the top of the cube converted at 180°C. In contrast, Figure 4c shows a

regular cell structure for the unconverted foam. The sample taken from the centre of the cube

converted at 180°C had a fairly regular cell structure (Figure 4b), much more reminiscent of
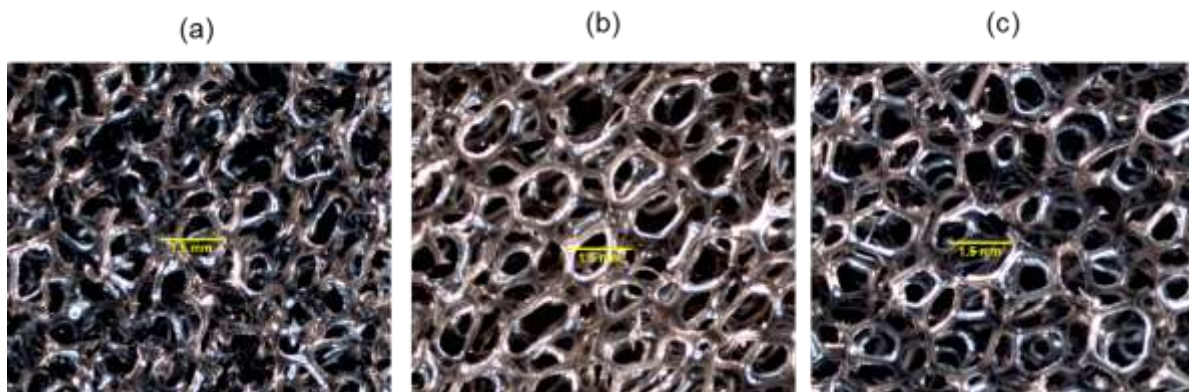
the unconverted foam structure.

Figure 4 Microscopic images of: a) Top sample of auxetic cube converted at 180°C, showing face corresponding to the outside of the trimmed cube, b) middle sample of auxetic cube converted at 180°C, c) unconverted open cell R30FR.

Figure 5a shows the VCR also changed through the cube, with lower levels of compression towards the centre. The VCR of all samples was lower than the applied value of 2.9, with the 180°C conversion showing the lowest levels of compression. Figure 5b shows Poisson's ratio also changed through the cube, further highlighting the inhomogeneous nature of the converted foams. The cube converted at 180°C had a lower Poisson's ratio for the top sample, which was more compressed and stiffer.
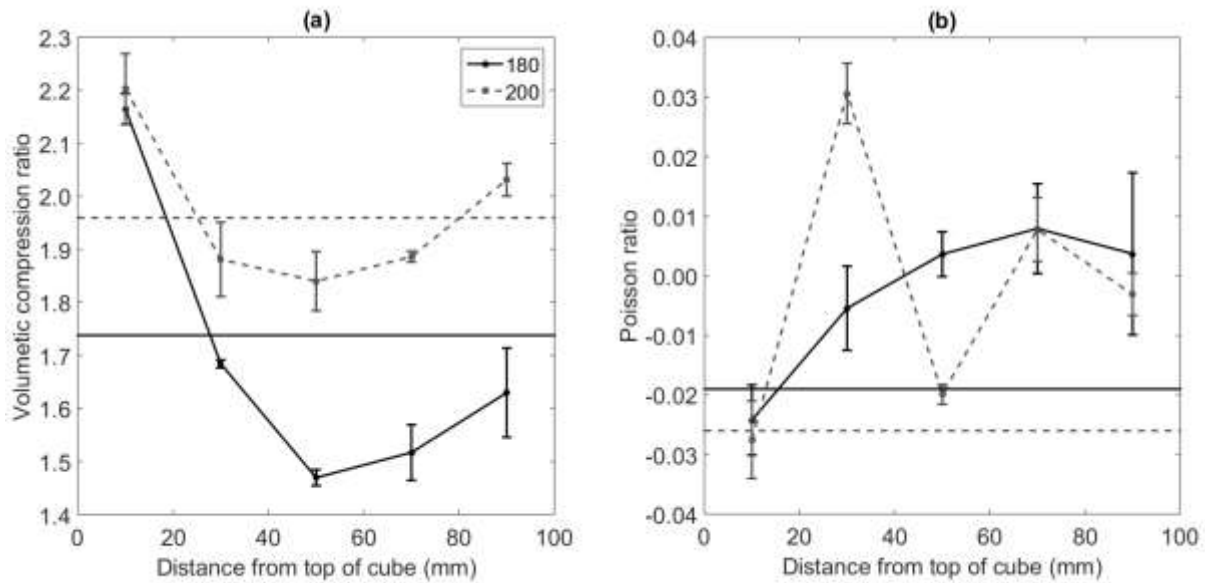
Figure 5 a) VCR and b) Poisson's ratio, with respect to position of the cuboid from the top of the cube. The horizontal lines correspond to the 100 x 100 x 100 mm cubes, error bars correspond to +/- 1 standard deviation.

Figure 6a show force-time plots for a 4 J impact on samples taken from the cube converted at 180°C, when covered with a 2 mm shell. The sample from the centre of the cube exhibited a sharp increase in force, and appears to have bottomed out. The sample taken from the top of the cube had a much more gradual loading profile and lower peak force. Figure 6b shows peak impact force for a 4 J impact on each 180°C sample with a 2 mm shell, normalised to the mean value obtained for unconverted foam samples with a 2 mm shell ($F_{normalised}=F_{sample}/F_{uc\ mean}$). Peak force for the auxetic sample taken from the top of the cube was ~10 times lower than the unconverted sample. In contrast, peak force was ~1.7-2.5 times lower for the other samples. Based on the results presented, only the top and bottom sample from the 200°C cube were used for further impact testing investigating the effect of covering sheet thickness.
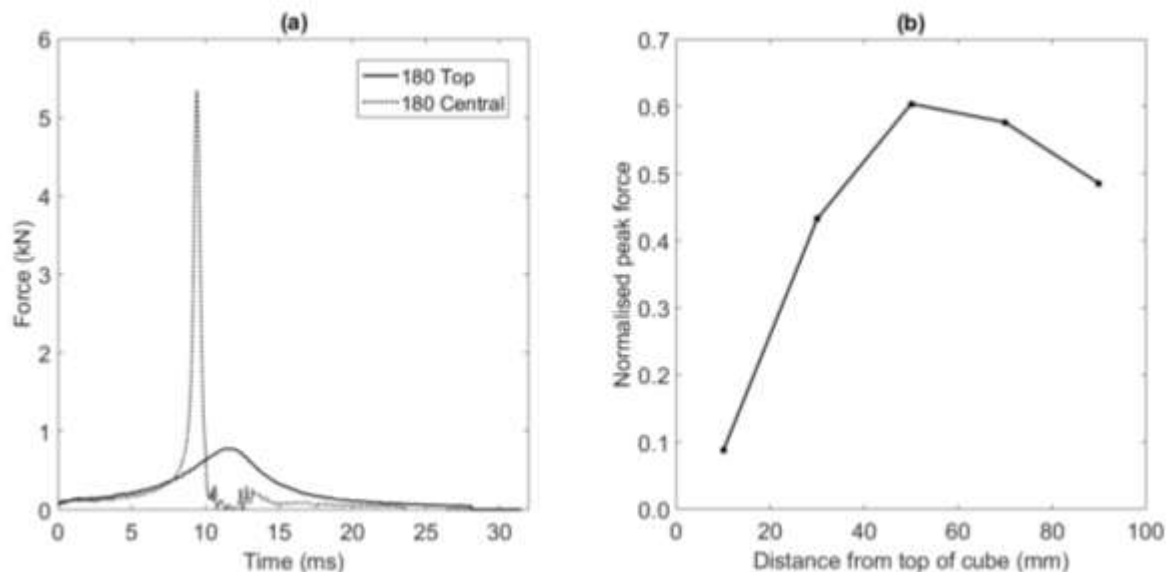
Figure 6 Results for 4J impacts on foam with 2 mm shell, a) Force-time curves for the top and central cuboidal slices from the 180°C cube b) Peak force normalised to the unconverted foam with respect to position of the cuboid from the 180°C cube. Unconverted peak force with 2 mm shell was 8850 ± 324 N for 4 J impacts.

Figure 7a shows force-time plots for a 4 J impact on the top cuboid from the 200°C cube and an unconverted sample, both with a 2 mm shell. The unconverted sample exhibited a sharp increase in force and appears to have bottomed out. The auxetic sample had a much more gradual loading profile and a peak force ~8 times lower, consistent with the results presented in Figure 6 for the 180°C top sample. Figure 7b shows force-time plots for auxetic samples with 1, 1.5 or 2 mm shells. The sample with the 1 mm shell appears to have bottomed out, with a peak force ~6 times higher than the test with the 2 mm shell. Based on these results neither unconverted samples nor auxetic samples with a 1 mm shell were tested above 4 J.
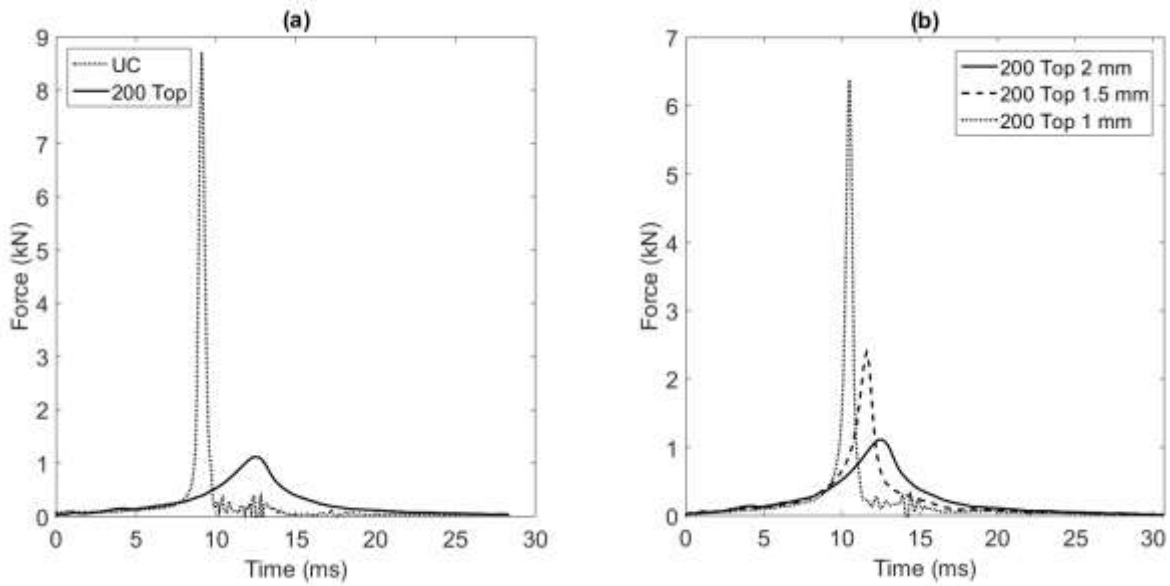
Figure 7 Force-time data for 4 J impacts; a) unconverted and auxetic with a 2 mm shell, b) auxetic with 1 mm, 1.5 mm and 2 mm shell. Auxetic corresponds to the top cuboid from the 200°C cube.

Figure 8 summarises peak force results for impacts on samples with different shell thicknesses at 4 and 6 J, normalised to the unconverted foam with a 1 mm shell at 4 J. Peak force was lower for auxetic samples than unconverted foam in all scenarios. Increasing shell thickness marginally reduced peak force for unconverted foam, while significantly reducing peak force for auxetic foam. For a 4 J impact, a 1 mm shell reduced peak force by <50% for auxetic foam in comparison to unconverted foam with the same thickness shell. Increasing shell thickness to 2 mm reduced peak force by >80% in comparison to unconverted foam in the same scenario. Peak forces for auxetic samples with a 2 mm shell impacted at 6 J were less than half those for the unconverted foam tested at 4 J. Once again, large variability in response is evident for auxetic samples taken from different locations of the same converted cube under identical test conditions.
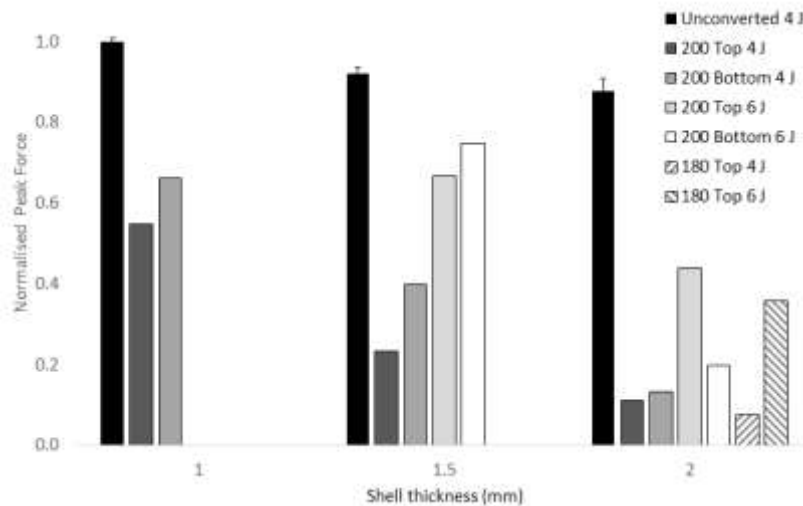
Figure 8 Peak force results normalised to the unconverted foam with a 1 mm shell at 4 J (10,082 ± 83 N). Error bars for the unconverted foam correspond to one standard deviation either side.

Discussion

A composite pad consisting of a 2 mm polypropylene sheet covering a 20 mm thick auxetic foam reduced peak force by ~10 times - for a 4 J impact from a rigid hemisphere - in comparison to the conventional counterpart. In contrast, placing a 1 mm sheet on each sample only resulted in the auxetic foam reducing peak force by <50%. Covering sheet properties clearly influence load distribution, deformation behaviour and impact performance of the underlying auxetic foam. Further work will investigate the effect of the mechanical properties of the sheet – thickness and material stiffness - on impact performance for a wider range of loading scenarios. Utilising a thin, stiff and high energy absorbing sheet - such as an auxetic carbon fibre-reinforced epoxy laminate [27] - will help keep pad thickness low.

Issues were observed when applying the thermo-mechanical conversion process to relatively large cubes of foam, resulting in an inhomogeneous material. Heterogeneous strain distributions have previously been observed in a coupled X-ray tomography and Digital Volume Correlation investigation into auxetic foams produced using the thermo-mechanical

conversion process [11], consistent with the inhomogeneous structure and properties reported in this work. The inhomogeneity arises due to issues of achieving uniform compression and temperature fields throughout the sample during conversion, and these are especially apparent as the sample size increases [8, 9, 18]. The inner regions of the cubes reported in this work were less compressed (lower VCR – Figure 5a) and had lower initial stiffness (Figure 3b), in agreement with previous work utilising a mechanical-chemical-thermal process [19]. The stress-strain curve for samples taken from the centre of a cube had a slight plateau region (Figure 3a), characteristic of a low level of compression during conversion [16] and consistent with less modification of the foam structure after conversion (Figure 4b). Samples taken from the top of a converted cube, on the other hand, had a higher level of volumetric compression (Figure 5a) and a stress-strain curve with an extended region of linear elasticity (Figure 3a) based on a re-entrant cell structure (Figure 4a), characteristic of auxetic foam [5, 15-17]. Impact tests confirmed superior force attenuation for the stiffer more compressed samples away from the centre of the cube (Figures 6 and 8), corresponding to the findings of previous work investigating different levels of compression during conversion [16].

The Poisson's ratio was measured in one plane only for each sample, with the foam rise direction aligned along the loading direction during testing. The directional dependency of Poisson's ratio in unconverted and converted foams has been considered in detail previously [28, 29]. Given the symmetry of the unconverted foam structure, the Poisson's ratio in the other orthogonal plane also having the foam rise direction in the loading direction is similar to that for the measuring plane reported here. The Poisson's ratio for loading of unconverted open cell thermoplastic foam in the foam rise direction differs to that for loading in one of the lateral directions (in the same plane as the foam rise direction) due to the elongated nature of the foam structure along the foam rise direction [28]. The Poisson's ratios in the transverse

plane (i.e. both loading and lateral directions perpendicular to the foam rise direction) may also be different to either of the on-axis Poisson's ratios in the planes containing the rise direction, again due to the anisotropy of the unconverted foam structure.

In the case of the converted foams, the effect of compression on the foam structure and, therefore, directional Poisson's ratio responses, depends on the nature of the compression applied during the conversion process. Highly anisotropic auxetic foams can be produced, for example, when the foam is biaxially compressed (transverse to the foam rise direction) [29]. Gradient foam structure and Poisson's ratio response can be produced by employing non-uniform compression along one or more axes during conversion [30]. Triaxial compression corresponding to the same level of compression along all three axes, as used in this work, generally leads to quasi-isotropic foam structure and Poisson's ratio response [5, 28, 29]. Hence the measurement of Poisson's ratio in one plane, with the loading direction corresponding to both the foam rise direction and the impact direction during the subsequent impact studies, is justified in the first instance. However, the previous studies have largely been confined to small converted cuboidal samples and so the effects of increased inhomogeneity reported above for the larger converted cubes merits further investigation in the future into the spatial variation of Poisson's ratio throughout the converted cubes, including in all three mutually orthogonal planes.

Further work will look to improve the conversion process to produce more homogeneous and better performing auxetic foam, simultaneously investigating the effect of applying different levels of compression, heating time and temperature and sample shape. Fabricating samples closer to the thickness required – rather than converting and slicing larger cubes – should achieve more uniform levels of compression and temperature during conversion. An

alternative solution to the temperature gradient may involve chemical conversion, or a mixed chemical and thermo-mechanical approach [12-13]. Despite outperforming conventional foam, auxetic samples showed an increase in peak force with impact energy from 4 to 6 J. Further work will, therefore, also investigate converting stiffer foams, and foams displaying larger magnitude of the negative Poisson's ratio, with the aim of producing improved auxetic foam at higher impact energies.

Through testing higher energy impacts on larger samples, the work presented here has shown further potential for auxetic foam to be applied to protective sports equipment. Auxetic foam considerably outperformed its conventional counterpart, in agreement with previous work [16-17]. Future work needs to focus on comparing auxetic foam with current materials and products, utilising an improved conversion process and a range of candidate materials. A consistent process for producing homogeneous samples of sufficient size for developing prototypes is needed, so these can be benchmarked against current products and relevant standards. Testing of auxetic foam should also extend to include tissues surrogates [e.g. 31] to provide impact scenarios which are more representative of those experienced by the human body. Finite element analysis has been applied to protective sports equipment [2-3]. Material models of auxetic foam under compression have been created [32], and future work will apply and implement this technique to further our understanding of how best to utilise auxetic foam. The Poisson's ratio and Young's modulus responses as a function of strain specific to the test specimen materials and dimensions employed in the impact tests reported here (e.g. Figure 3b for tangent modulus) will be utilised in these modelling investigations.

Conclusion

Open-cell auxetic foam covered with a thin shell exhibited higher force attenuation than the

conventional counterpart, when impacted with a rigid hemisphere. Increasing shell thickness had little effect on the conventional foam but resulted in considerably improved performance for the auxetic foam. Future work should investigate shell properties in more detail for a range of impact scenarios. Large variations within converted samples warrant further work to improve the conversion process. Larger sized samples now need to be produced so prototypes can be developed and tested against current products.

Acknowledgements

References

[1]   Hrysomallis C 2009 Surrogate thigh model for assessing impact force attenuation of protective pads *Journal of Science and Medicine in Sport* 12 35-41

[2]   Ankrah S and Mills N J 2003 Performance of football shin guards for direct stud impacts *Sports Engineering* 6 207-219

[3]   Ankrah S and Mills N J 2004 Analysis of ankle protection in Association football *Sports Engineering* 7 41-52

[4]   Mills N J 2003 Foam protection in sport *Materials in sports equipment Vol. 1* edited by Jenkins M J (Woodhead, Cambridge)

[5]   Lakes R 1987 Foam structures with a negative Poisson's ratio *Science* 235 1038-1040

[6]   Bezazi A, & Scarpa F 2007 Mechanical behaviour of conventional and negative Poisson's ratio thermoplastic polyurethane foams under compressive cyclic loading *International Journal of fatigue* 29 922-930

[7]   Lim T C 2015 *Auxetic Materials and Structures* Springer pp55-56

[8]   Critchley R, Corni I, Wharton J A, Walsh F C, Wood R J and Stokes K R 2013 A review of the manufacture, mechanical properties and potential applications of auxetic foams

physica status solidi (b) 250 1963-1982

[9]   Chan N and Evans K E 1997 Fabrication methods for auxetic foams *Journal of Materials Science* 32 5945-5953

[10]   Lim T C, Alderson A and Alderson K L 2014 Experimental studies on the impact properties of auxetic materials *physica status solidi (b)* 251 307-313

[11]   Pierron F, McDonald S A, Hollis D, Fu J, Withers P J and Alderson A 2013 Comparison of the Mechanical Behaviour of Standard and Auxetic Foams by X-ray Computed Tomography and Digital Volume Correlation *Strain* 49(6) 467-482

[12]   Grima J N, Attard D, Gatt R and Cassar R N 2009 A novel process for the manufacture of auxetic foams and for their re-conversion to conventional form *Advanced Engineering Materials* 11 533-535

[13]   Lisiecki J, Błażejewicz T, Kłysz S, Gmurczyk G, Reymer P, and Mikułowski G 2013 Tests of polyurethane foams with negative Poisson's ratio *physica status solidi (b)* 250 1988-1995

[14]   Friis E A, Lakes R S and Park J B 1988 Negative Poisson's ratio polymeric and metallic foams *Journal of Materials Science* 23 4406-4414

[15]   Sanami M, Ravirala N, Alderson K and Alderson A 2014 Auxetic materials for sports applications *Procedia Engineering* 72 453-458

[16]   Allen T, Shepherd J, Hewage T A M, Senior T, Foster L and Alderson A 2015 Low-kinetic energy impact response of auxetic and conventional open-cell polyurethane foams *physica status solidi (b)* 252, No. 7, 1631–1639

[17]   Allen T, Martinello N, Zampieri D, et al. 2015 Auxetic foams for sport safety applications *Procedia Engineering*

[18]   Lowe A and Lakes R S 2000 Negative Poisson's ratio foam as seat cushion material *Cellular Polymers* 19 157-168

[19]   Lisiecki J, Kłysz S, Błażejewicz T, Gmurczyk G and Reymer P 2014 Tomographic examination of auxetic polyurethane foam structures *physica status solidi (b)* 251 314-320

[20]   Lakes RS and Elms K. Indentability of conventional and negative Poisson's ratio foams. J Compos Mater 1993; 27: 1193–1202.

[21]   Gibson L J and Ashby M F 1997 *Cellular solids: structure and properties* (Cambridge: Cambridge University Press)

[22]   Masters I and Evans K 1996 Models for the elastic deformation of honeycombs Composite structures, 35(4), pp. 403-422.

[23]   Chan N and Evans K E 1998 Indentation resilience of conventional and auxetic foams *Journal of cellular plastics* 34 231-260

[24] Pastorino P, Scarpa F L, Patsias S, Yates JR, Haake SJ and Ruzzene M 2007 *Strain rate dependence of stiffness and Poisson's ratio of auxetic open cell PU foams* physica status solidi (b) 244(3) pp 955 - 965

[25] BS 6183-3 2000 *Protective equipment for cricketers-leg protectors for batsmen, wicket-keepers and fielders, and thigh, arm and chest protectors for batsmen*. British Standards Institute.

[26]   Hertz H 1881 *J. Maths (Crelle J)* 92

[27]   Alderson K L and Coenen V L 2008 The low velocity impact response of auxetic carbon fibre laminates *physica status solidi (b)* 245 489-496

[28]   Chan N and Evans K E 1999 The Mechanical Properties of Conventional and Auxetic Foams. Part I: Compression and Tension *Journal of Cellular Plastics* 35 130-165

[29]   Alderson A, Alderson K L, Davies P J and Smart G M 2005 The effects of processing on the topology and mechanical properties of negative Poisson's ratio foams Proc. ASME Int. Mechanical Engineering Congress and Exposition (Aerospace Division) (Orlando, FL, Nov. 2005) vol 70AD p 503

[30]   Sanami M, Alderson A, Alderson K L, McDonald S A, Mottershead B and Withers P

J 2014 The production and characterization of topologically and mechanically gradient open-

cell thermoplastic foams *Smart Mater. Struct.* 23 055016 (13pp)

[31]   Payne T, Mitchell S, Bibb R and Waters M 2015 Development of novel synthetic

muscle tissues for sports impact surrogates *Journal of the mechanical behavior of biomedical*

materials 41 357-374

[32]   Ciambella J, Bezazi A, Saccomandi G and Scarpa F 2015 Nonlinear elasticity of

auxetic open cell foams modeled as continuum solids *Journal of Applied Physics* 117 184902